

Investigation of blind massive sulphide deposit signatures in the calcrete layers as a geochemical barrier: A case study of Areachap, Kantienpan and Copperton deposits

R.Ghavami-Riabi^{1*}; and H.F.J. Theart²

1. Faculty of Mining, Petroleum and Geophysics, Shahrood University of Technology, Shahrood, Iran

2. SRK Consulting Engineers and Scientists, 265 Oxford Road, Ilovo, Johannesburg, South Africa

Received 8 Sep 2011; received in revised form 20 Dec 2011; accepted 5 Apr 2012

*Corresponding author: rghavami2@yahoo.com (R. Ghavami-Riabi).

Abstract

The trace element contents on the surface originated from mineralization would depend to the thickness of the calcrete layer above the ore deposit on the surface. A very thick layer of calcrete may not allow for much dispersion of the elements of interest in the surface. These elements may be concentrated in non-magnetic and magnetic part of calcrete. Based on the current research, mineralogical composition of the non-magnetic part of the calcrete consists of calcite, quartz and microcline and the magnetic part comprises of magnetite, hematite, calcite and albite (at Kantienpan). It could be demonstrated that calcrete samples close to the ore zone have higher contents of Cu, Zn and CaCO₃ when compared to the calcrete samples further away from the ore zone. Litho-geochemical exploration program based on the visually cleaned calcrete samples may lead to the successful identification of underlying mineralization, but the dispersion of the interest elements may be severely restricted. It is however evident that these elements are available at the calcrete-sand interface and could then be dispersed by ground and rain water as in the case of mobile metal ions.

Keywords: *Calcrete; massive sulphide; VHMS; mobile metal ion*

1. Introduction

A calcrete layer forms near the surface by evaporation of soil moisture during the diurnal cycle (under arid to semi-arid conditions). Khadkikar et al. (2000) classified calcretes into three groups based on the processes of formation, pedogeniccalcrete (soil-forming), groundwater calcrete (groundwater processes) and calcrete conglomerate (reworking of both groups). The groundwater calcrete or non-pedogeniccalcrete is formed by carbonate-bearing groundwater circulating through sediments during dry seasons [1, 2]. During these dry periods, groundwater with

dissolved carbonates rises through the host sediments by capillary action. As the groundwater reaches the surface, evaporation will cause precipitation of carbonate close to or on the surface resulting in the formation of calcrete. Pedogeniccalcrete develops in more arid areas where rainfall only moisturizes the soil and creates a soil moisture zone during wet seasons. The dissolved carbonates move through the soil moisture zone and are precipitated on the surface by evaporation during dry seasons [1, 2]. Calcrete may also form due to the interaction of plant root

growth, water and the erosion-sedimentation processes [3]. This type of calcrete is known as biogenic or β -calcretes and does not form layers. When water is available, high soil moisture may favour rapid plant colonisation. The plant would absorb the carbonate bearing groundwater via its roots [3]. As the plant uses up the water, the carbonate is left behind to accumulate forming round micritic calcite particles. Khadkikar et al. (1998) introduced rhizogenic calcretes, which are calcretes formed by physiochemical processes in the root zone. The plant root uptakes the water causing the remaining soil water to be super saturated in Ca^{2+} ions [4].

Calcrete, known as caliche, croutes, calcaires, nari and kunkar, is a predominantly calcium carbonate component. Calcrete may form in arid (50-100 mm mean annual rainfall) to sub-humid (500-700 mm mean annual rainfall) conditions [5, 3] and the existence of calcrete in an area is evidence for dry periods, where evaporation exceeds precipitation. Calcretes are mostly composed of calcite, quartz and feldspar [1], with the silica content affecting the hardness of calcretes, i.e. the higher the silica content, the harder the calcrete. Aragonite and calcium carbonate-hydrate minerals may be present in the early stages of calcrete formation. Dolomite (dolocrete) may also occur together with calcite [1]. Khadkikar et al. (1998; 2000) reported on the presence of clay minerals and trace amount of gypsum and barite in some calcretes. In drier climates (50-100 mm average annual rainfall), sepiolite and palygorskite are usually formed [3].

The absence of sepiolite-palygorskite and the presence of smectite and hematite associated with low Mg calcite are characteristics of calcretes formed in semi-arid climates (100-500 mm average annual rainfall) [3]. The formation of pedogenic hematite requires enough moisture to enable chemical weathering of primary minerals and low activity of water that would propel dehydration processes like in the tropical environments [5, 3].

During rainfall, acidic water percolates into the soil, and it carries dissolved CO_2 from river water as well as the aeolian dust. In the event that there is an ore body close to surface, the carbonate-bearing water will react with the ore body resulting in “mobile elements” in the ore body being dissolved. Later, evaporation processes take place and result in the solution rising to the surface by capillary action. The convection cells are set up by rainfall and evaporation during the rainfall and dry periods (Figure 1). “Mobile Metal Ions” have the ability to disperse through un-mineralized rock e.g. hundreds of meter vertically upwards possibly by poorly understood micro-bubbles, vapor, ground-water flow, capillary rise or electrochemical processes [6, 7].

Mann et al. (1995) and Mann et al. (1997) carried out experimental work to determine the vertical movement of mobile elements and the effect a calcium carbonate layer would have on the movement of these mobile ions. In the first experiment (without addition of calcium carbonate),

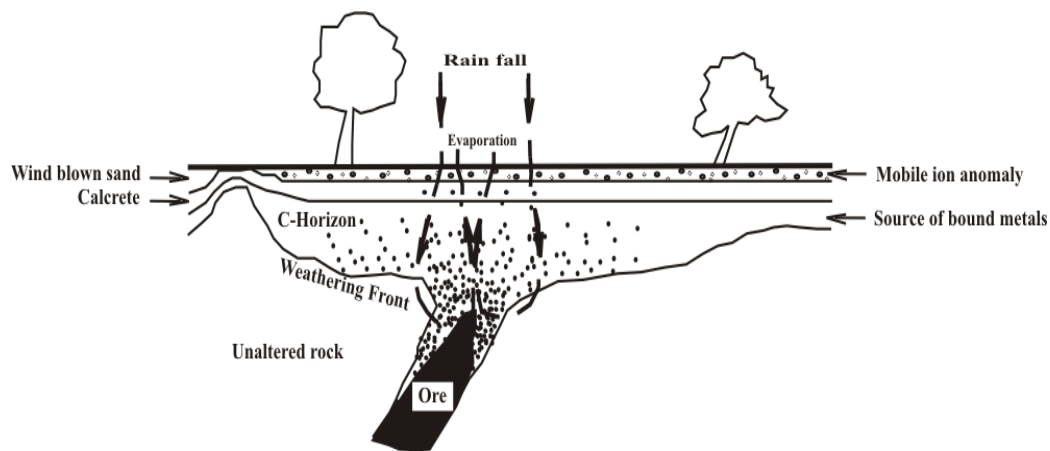


Figure 1. Schematic model of convection cell in connection with mobile metal ions in the secondary environment (after Mann et al., 1997)

coarse silica sand was added to a flower pot partially filled with a solution containing base metals. The metals in the solution were shown to move vertically upwards through the silica sand in a very short period [8, 9]. In the second experiment, varying quantities of calcium carbonate were added as a single layer to a pot with a solution and coarse silica sand as in the first experiment. In both experiments, i.e. with or without carbonate added, a surface accumulation of mobile metals was observed. Thus it suggests that carbonate, a known precipitant of base metals, has not inhibited the surface response or the movement of the base metals [8, 9].

The calcrete layer, as part of the secondary environment, is investigated in the current paper by samples collected from surface and at different depths in the calcrete layer to investigate the variation in the concentration of some trace elements in this potential barrier to geochemical dispersion. The objective of this research is to determine whether a litho-geochemical survey of calcrete samples would be successful in detecting underlying massive sulphide mineralization.

2. Geological condition of the study area

The calcrete layers at the base of the Kalahari Group formed during a dry period that existed during the later part of the Tertiary Period [10], more specifically during the late Miocene Epoch (23.8-5.3 Ma) [11]. Different formations of the Kalahari Group were studied by Malherbe (1984) (Table 1). The Mokalanen Formation, which is the calcrete unit of the Kalahari Group, comprises of three units and two varieties of calcrete layers, namely nodular and hardpan calcretes. The hardpan calcrete is hard and impermeable and forms when

the nodular calcrete is cemented by calcrete or silcrete. It provides evidence of the semi-arid environmental conditions during the formation of the Mokalanen Formation. The hardpan calcrete is an extremely weathering-resistant rock. The calcrete layer developed near the surface throughout the study area from Areachap in the north to Copperton in the south (Figure 2) is correlated with Malherbe's (1984) Mokalanen Formation.

Vermaak (1984) suggested a pedogenic process for the formation of the calcrete at Areachap, Copperton and Jacomynspan areas. A non-pedogenic, groundwater, process was suggested by Nash and McLaren (2003) for the Kalahari valley calcrete in the capillary fringe zone of the groundwater table. Based on the semi-arid environmental conditions proposed by Malherbe (1984) during the formation of the Mokalanen Formation, classification of calcrete by Khadkikar et al. (2000) and average of rainfall in the study area, a pedogenic origin may be accepted for these calcretes.

3. Sampling and analytical methods

The objective of sampling the calcrete was to investigate if the metals may remain sufficiently mobile in the groundwater of the secondary environment and transport to the surface under the high pH condition. For this propose, the variations in the concentration of the elements of interest in the calcrete layer are investigated with depth.

In the study area, a layer (of variable thickness ranging from zero to several meters) of wind blown sand covers the calcrete layer that in itself varies from zero to 6 m or more [12].

Table 1. Different Formations of the Kalahari Group. Data summarised from Malherbe (1984)

| Name of the Formation | Lithologies in the Formation |
|------------------------|---|
| Gordonia Formation | Sand dune deposits and Fe-rich minerals such as magnetite, haematite and Ilmenite |
| GoeboeGoeboe Formation | Sand sediment |
| Lonely Formation | Clayey diatomaceous limestone |
| Mokalanen Formation | - Harden calcrete -Nodular calcrete -Sharpstonecalc-conglomerate |
| Eden Formation | Sandstones and conglomerate |
| Budin Formation | Red clay |
| Wessels Formation | Gravel |

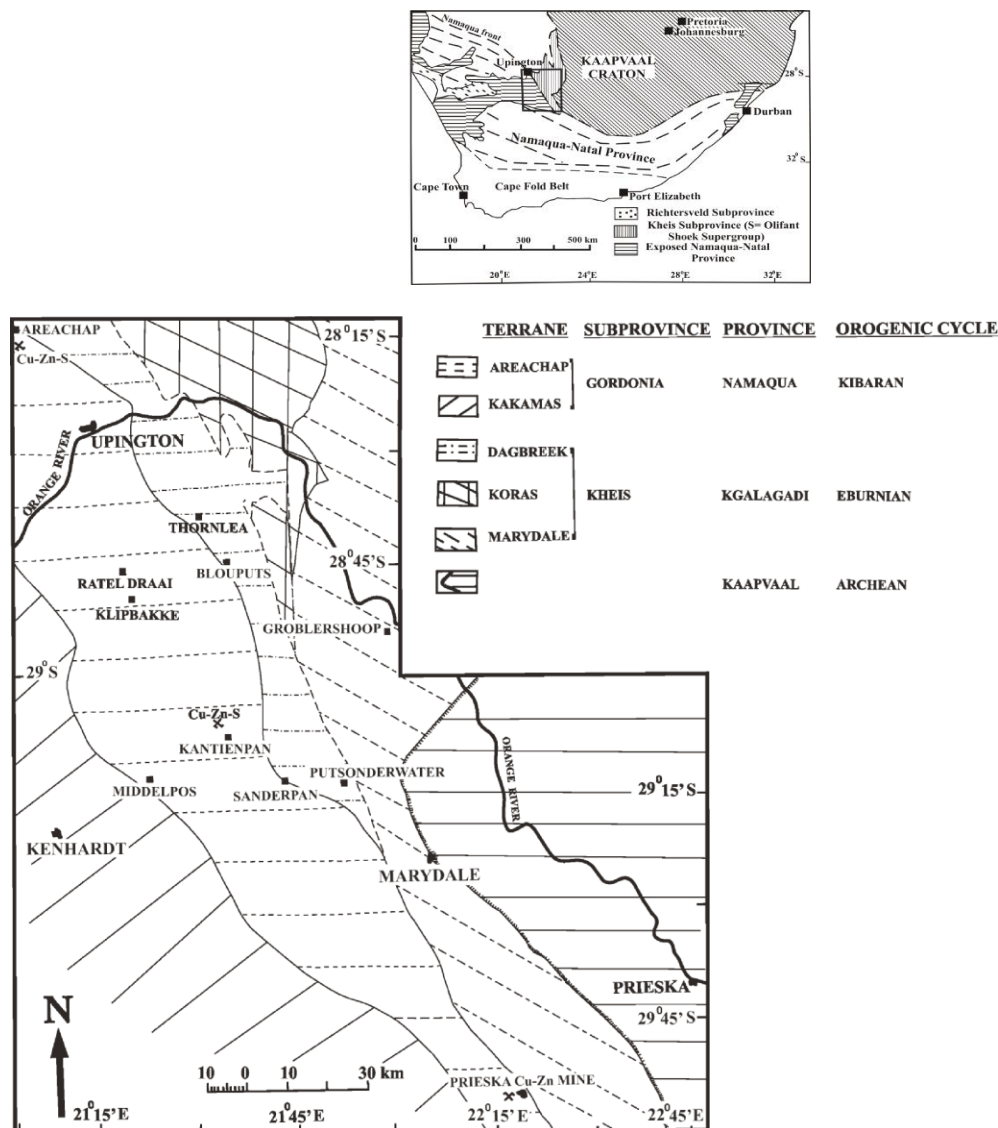


Figure 2. The location and geological map of the Areachap Group in the eastern part of Namaqua Sub-province.

A total of 14 samples, approximately 3 kg each, were collected from the calcrete layer in the two areas under investigation. Six calcrete samples were collected from the surface near the gossan zone at Kantienpan (Figure. 3), together with two calcrete samples (outside the Kantienpan geology map) further away from the ore zone. Except these two samples, the rest of the samples collected from directly above the ore zones contained inclusions of gossan materials.

Six calcrete samples were collected in two depth profiles, from an old excavation at Areachap (Figure 4), each profile includes three samples (Figure 5). A gossan zone with malachite-filled veinlets occurs at the bottom of this layer (Figure

5C). The gossan zone display fractures filled with what appears to be Dwykatillite at Areachap. If this is the case, it would imply that the gossan formed before the denudation as a result of the glaciation at the onset of the Karoo sedimentation.

A Frantz isodynamic magnetic separator was used to separate the magnetic part of calcrete samples by varying the electric current flowing through the electromagnet (Figure A.1). Mineralogical phases in the magnetic and non-magnetic parts of one sample (KP12/4) were determined by x-ray diffractometry (XRD) and element concentrations in the magnetic, non-magnetic and original samples were analyzed by XRF.

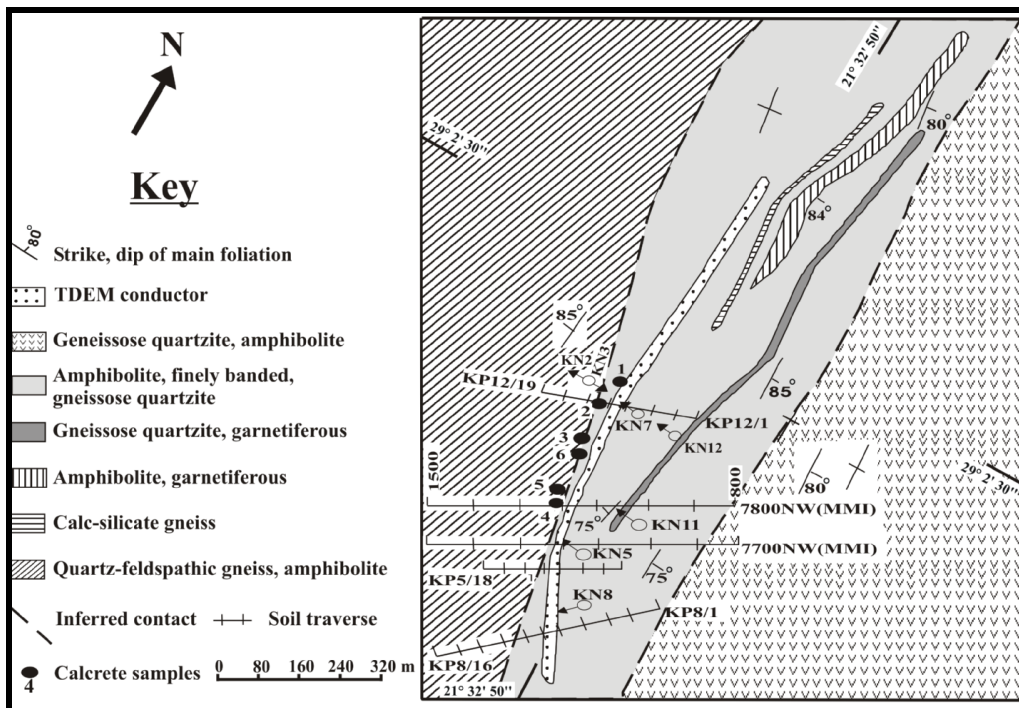


Figure 3. Location of calcrete samples and geology map of the Kantienpan area (after Rossouw, 2003)

4. Source of mineralized elements

The current investigation intends to further study Vermaak (1984) on the calcretes by establishing the actual host of the elements of interest such as Cu, Zn, Pb and S in the calcrete environment. The question asked is if these elements are dispersed into the calcrete itself, or if they are confined to the distribution of gossan inclusions. Should the former be the case, calcrete may have to be sampled in future geochemical exploration programmes. In this regard it is important to refer to the study of McQueen et al. (1999) where it was found that Au could be found in the low Mg-calcite of calcrete from southeastern Australia [18, 19, 20].

The calcrete of the study area is mainly composed of a calcite (low Mg), and quartz as determined by XRD (Table 2). The non-magnetic part of the sample contains calcite, quartz and alkali feldspars, whereas the magnetic part of sample comprises calcite and some quartz and alkali feldspars together with the hematite and magnetite minerals (Table 2). This is most probably due to the difficulty of liberating the different minerals in the calcrete material. Table 2 demonstrates that albite and microcline are concentrated in the non-magnetic fractions. Calcite is present in both the magnetic and non-magnetic fractions of the sample. Relative to

calcite, quartz, is more abundant in the nonmagnetic fraction.

Magnetite and hematite, presumably related to the gossan component of the sample, are extracted in the first and second magnetic separates. Ilmenite and actinolite are present in the higher current magnetic fractions of the calcrete sample in very low concentrations.

The calcite is expected to buffer surface water at relatively high pH conditions and therefore lower the solubility of base metals, limiting the mobility of these elements (Cu, Zn and Pb). Mann et al. (1995) and Mann et al. (1997) have shown that varying quantities of calcium carbonate placed artificially as a single layer on top of sand do not prevent the solution from transmitting a base metal anomaly from the underlying material to the overlying sand. In the current study, this finding is tested under natural conditions where the anomaly related to the weathered massive sulphide deposit is separated from overlying eolian sand by a calcrete layer of substantial thickness.

To investigate the mobility of the elements of interest in the calcrete, it is important to discriminate between the base metals contained in gossan clasts in the calcrete and those dispersed in the calcrete itself.

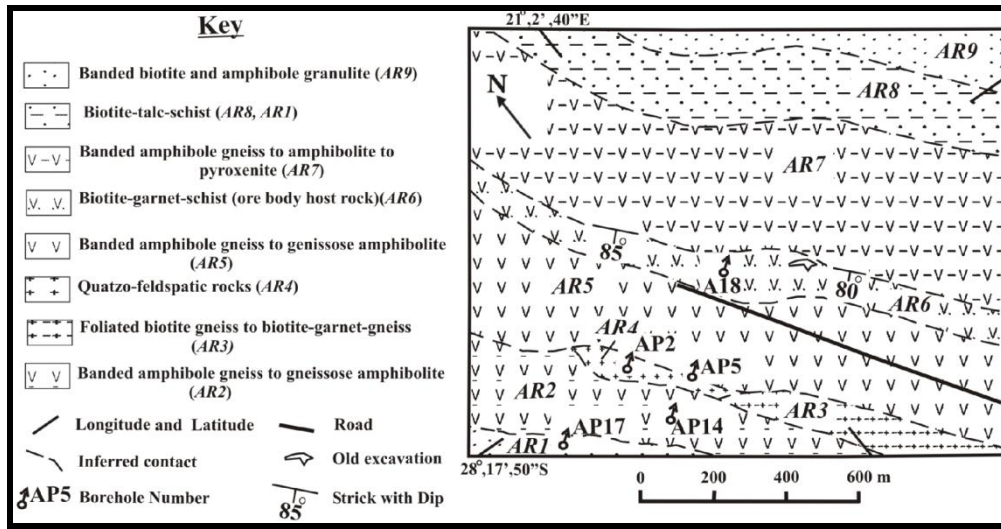


Figure 4. Location of old excavation and geological map of the Areachap area (after Voet and King, 1986).



Figure 5. The calcrete layer in an old excavation at Areachap. Calcrete profile Calc1 (A), Calc2 (B) and a gossan rock with malachite and calcrete-filled veinlets at the bottom of calcrete layer (C).

Two possible ways by which the calcrite and gossan fragments could be investigated separately were considered here, namely selective dissolution and physical separation using magnetic properties.

Because of the potential contamination of the chemical solutions it was decided to investigate the dispersion of the ore related elements in the calcite part of the calcrite.

Table 2. Different minerals in the visually cleaned, magnetic and non-magnetic parts of a calcrite sample (KPR12/4, Kantienpan) as determined by quantitative XRD.

| Sample | Cal | Q | Mc | Ab | Ms | Ilm | Hem | Mgt | Act |
|------------------|-------|-------|------|------|------|------|------|------|------|
| KPR12/4 | 77.09 | 13.10 | 2.84 | 4.20 | 2.78 | - | - | - | - |
| Non-Mag 1 | 75.59 | 12.17 | 5.51 | 4.96 | 1.77 | - | - | - | - |
| Non-Mag 2 | 75.15 | 11.69 | 6.45 | 4.39 | 2.32 | - | - | - | - |
| Non-Mag 3 | 73.21 | 13.91 | 6.05 | 4.72 | 2.11 | - | - | - | - |
| Mag 1 | 77.24 | 10.36 | 5.61 | 4.89 | 1.55 | - | - | 0.35 | - |
| Mag 2 | 78.04 | 9.75 | 4.85 | 1.88 | 0.87 | - | 1.73 | 2.56 | - |
| Mag 3 | 77.92 | 9.24 | 3.93 | 5.05 | 2.09 | 0.9 | - | - | 0.44 |
| Mag 4 | 78.89 | 7.52 | 3.75 | 5.93 | 1.88 | 0.87 | - | - | 1.17 |
| Mag 5 | 75.65 | 8.70 | 5.78 | 6.46 | 2.89 | 0.23 | 0.29 | - | - |

Cal: calcite, Q: quartz, Mc: microcline, Ab: albite, Ms: muscovite, Ilm: Ilmenite, Hem: hematite, Mgt: magnetite, and Act: Actinolite

It is unpractical to determine the concentrations of elements of which the abundances are in the parts per million ranges by microprobe analysis. It was therefore decided to analyze the calcrite by XRF after the physical separation of the calcite rich portion from the gossan rich material. For this purpose, the magnetic component of the calcrite sample was separated first by hand sorting and then by using a hand magnet followed by a Frantz isodynamic magnetic separator (see Figure A.1, for detail). The results of the XRF analysis on the magnetic and non-magnetic parts of sample KP12/4 are shown in Table A.2. It is assumed that most of the Ca and Mg present in the sample would be in a carbonate form and the Ca and Mg contents (normally expressed as oxides) were recalculated as carbonates.

4.1. Kantienpan calcrite samples

The fact that the recalculated total sum of major elements shown in Table 3 is much closer to the ideal 100% shows that this is a valid assumption. These samples contain 70.25 to 75.75% CaCO₃, 12.4 to 18.4% SiO₂, 0.74 to 10% Fe₂O₃, 5.04 to 5.83% MgCO₃ and 1.9 to 2.7% Al₂O₃ as based on semi-quantitative major element XRF powder analyses. In terms of trace elements, non-magnetic parts (sample Non-Mag1 and 3) have the highest concentration of S (Table 3). However, in some of the other samples higher S contents were observed

in the magnetic fractions (KP12/2 and KP12/3, Table 4) and it must be concluded that the results on the S distribution remains inconclusive. The magnetic separate has higher Zn, Cu, Pb and V contents when compared to the original and non-magnetic samples (Table 3). Based on the results of this table, the Frantz isodynamic magnetic separator did not give a significant improvement on the purity of the calcite rich material separated visually. The sample cleaned with the Frantz separator (Non-Mag 1 and 2) does not result in a marked improvement when its composition is compared with the visually cleaned sample (KP12/4, after hand separation). It was decided to use only visually cleaned calcrite material for further investigation, since these results would also be easy to reproduce and cost efficient during an exploration campaign.

Cu is associated with the iron oxides, but seems to be dispersed in the rest of the sample as well. This conclusion is substantiated by the results of the other samples (Tables 2 and 3), showing that Cu may be concentrated in the hematite/magnetite (iron rich) components of the samples. Distribution of Zn appears to be more strongly related to the distribution of magnetite, although some of the Zn may also be dispersed in the other iron-bearing fractions of the sample. Pb may be directly associated with the distribution of magnetite in Table 3. However the abundance of Pb is low in the other samples and no significant conclusion could be reached. Finally, the distribution of V appears to be strongly related to the distribution of magnetite (Tables 2 and 3).

Table 3. Comparison of major and trace elements of interest in visually cleaned, magnetic and non-magnetic parts of calcrete sample KP12/4, Kantienpan (A: ampere)

| Major (%) | Visually clean KPR 12/4 | Non-magnetic part of sample | | | Magnetic part of sample | | | | |
|----------------------------------|-------------------------------|-----------------------------|--------------|--------------|-------------------------|---------------|--------------|--------------|--------------|
| | | Completely clean | | Clean1 | Hand magnet | 0.1A | 0.3A | 0.5-0.9A | 1.1-1.7A |
| | | Non-Mag1 | Non-Mag2 | Non-Mag3 | Mag1 | Mag2 | Mag3 | Mag4 | Mag5 |
| CaCO ₃ * | 70.25 | 71.09 | 75.00 | 71.36 | 75.75 | 71.29 | 72.80 | 72.73 | 72.46 |
| SiO ₂ * | 18.43 | 16.84 | 13.84 | 15.56 | 12.67 | 12.71 | 12.42 | 13.79 | 14.69 |
| TiO ₂ * | 0.22 | 0.09 | 0.1 | 0.15 | 0.21 | 0.51 | 1.1 | 0.98 | 0.53 |
| Fe ₂ O ₃ * | 1.52 | 0.74 | 0.74 | 1 | 1.61 | 9.99 | 3.2 | 3.3 | 2.14 |
| MgCO ₃ * | 5.35 | 5.04 | 4.90 | 5.26 | 5.09 | 5.64 | 5.14 | 5.62 | 5.83 |
| Al ₂ O ₃ * | 2.54 | 1.99 | 1.91 | 2.05 | 1.91 | 1.92 | 1.94 | 2.35 | 2.66 |
| Na ₂ O * | 0.23 | 0.24 | 0.24 | 0.23 | 0.23 | 0.27 | 0.27 | 0.28 | 0.28 |
| K ₂ O * | 0.71 | 0.66 | 0.58 | 0.64 | 0.57 | 0.41 | 0.44 | 0.49 | 0.56 |
| TOTAL | 99.25 | 96.69 | 97.31 | 96.25 | 98.04 | 102.74 | 97.31 | 99.54 | 99.15 |
| Trace elements (ppm) | | | | | | | | | |
| Cu | 20 | 12 | 8 | 12 | 5 | 6 | 11 | 14 | 13 |
| Pb | 4 | 3 | 3 | 6 | 3 | 16 | 3 | 4 | 3 |
| Zn | 45 | 42 | 39 | 52 | 42 | 70 | 86 | 68 | 62 |
| S * | 513 | 578 | 363 | 1142 | 446 | 289 | 300 | 299 | 329 |
| V | 35 | 16 | 18 | 19 | 37 | 305 | 72 | 63 | 46 |

Note: KPR12/4 is the original sample, *: semi-quantitative analysis, 1: Cleaned by hand magnet

The variation of major oxides and trace elements for the visually cleaned calcrete samples taken from the surface at Kantienpan are given in Table 4. These samples contain 70.25 to 83.27 % of CaCO₃, 9.4 to 18.43 % SiO₂, 1.22 to 2.54 % Al₂O₃, 4.15 to 6.07 % MgCO₃ and 0.79 to 2.31 % Fe₂O₃ contents based on semi-quantitative XRF powder analyses. Samples KP12/3 and KP12/6 are from the gossan-bearing zone, and shown the highest Cu, Zn, S and V contents as determined by quantitative (Cu, Zn and V) and semi-quantitative (S) XRF analyses.

4.2. Areachapcalcrete samples

Figure 6 shows the variation of major oxides (based on XRF analysis) in the cross-section at Areachap versus depth for the non-magnetic parts of the original samples (visually clean calcrete). The variation of CaCO₃ verse depth differs from the other component (Figure 6). They are composed of 54.98 to 83.34 % CaCO₃, 10 to 26.52 % SiO₂, 1.43 to 6.24 % Al₂O₃, 3.36 to 5.69 % MgCO₃ and 0.91 to 4.77 % Fe₂O₃ based on semi-quantitative XRF powder analyses.

The variations of Cu, Zn, Pb and S as determined by quantitative (Cu, Zn and Pb) and semi-quantitative (S) XRF analyses versus depth in original calcrete samples (visually clean calcrete) for the same sample profile (Calc1) are shown in Figure 7. Based on this figure, Cu, Zn and Pb contents increase with depth. The concentrations of these elements are

therefore much lower at surface than deeper down the calcrete profile. It may be concluded that the peak to background ratio of anomalies in surface samples would depend on the thickness of the underlying calcrete layer. S does not show the same trend as Cu, Zn and Pb. This may be explained by the presence of different types of sulphur phases in the sample, i.e., sulphates as a result of ground water compositions and the evaporation processes and sulphates as remnants of the oxidised primary sulphide minerals. It should also be considered that sulphates may accumulate in the surface environment due to the interaction of rain water, groundwater and evaporation processes such as seen in pan formation. This may result in false S anomalies not related to underlying sulphide mineralization.

Figures 6 and 7 display an increasing trend of trace elements (Cu, Zn and Pb) and major oxides such as Al₂O₃, MgCO₃, SiO₂ and Fe₂O₃ with depth. This may be seen as evidence that the calcrete formation was superimposed on a weathered soil profile and that the calcrete does not merely represent calcretized Kalahari sand. This interpretation is also supported by the observation that gossanclasts are enclosed directly above the ore zone in the calcrete over the entire thickness of the calcrete layer. It is expected that the primary mineral phases would be the same as determined for Kantienpan namely calcite, quartz, albite and microcline.

Table 4. The comparison of major oxides and trace elements of interest in visually cleaned parts of calcrete samples in the Kantienpan (*: semi-quantitative analyses)

| Major elements(%) | Visually clean calcrete samples | | | | | |
|----------------------|---------------------------------|---------------|---------------|--------------|--------------|---------------|
| | Major oxides (%) | | | | | |
| | KPR12/1 | KPR12/2 | KPR12/3 | KPR 12/4 | KPR12/5 | KPR12/6 |
| CaCO3 * | 77.32 | 78.88 | 83.27 | 70.25 | 70.93 | 79.20 |
| SiO2 * | 14 | 11.79 | 9.44 | 18.43 | 16.59 | 11.34 |
| TiO2 * | 0.1 | 0.15 | 0.12 | 0.22 | 0.19 | 0.16 |
| Fe2O3 * | 0.79 | 1.48 | 1.54 | 1.52 | 2.31 | 3.05 |
| MgCO3 * | 6.02 | 6.07 | 4.15 | 5.35 | 5.95 | 4.15 |
| Al2O3 * | 1.22 | 1.68 | 1.23 | 2.54 | 2.42 | 2.01 |
| Na2O * | 0.18 | 0.19 | 0.19 | 0.23 | 0.24 | 0.2 |
| K2O * | 0.33 | 0.51 | 0.29 | 0.71 | 0.72 | 0.45 |
| TOTAL | 99.96 | 100.75 | 100.23 | 99.25 | 99.35 | 100.56 |
| Trace elements (ppm) | | | | | | |
| Cu | 9 | 19 | 32 | 20 | 17 | 49 |
| Pb | 3 | 5 | 9 | 4 | 7 | 4 |
| Zn | 40 | 95 | 117 | 45 | 62 | 210 |
| S* | 532 | 488 | 601 | 513 | 469 | 495 |
| V | 26 | 28 | 28 | 35 | 37 | 60 |

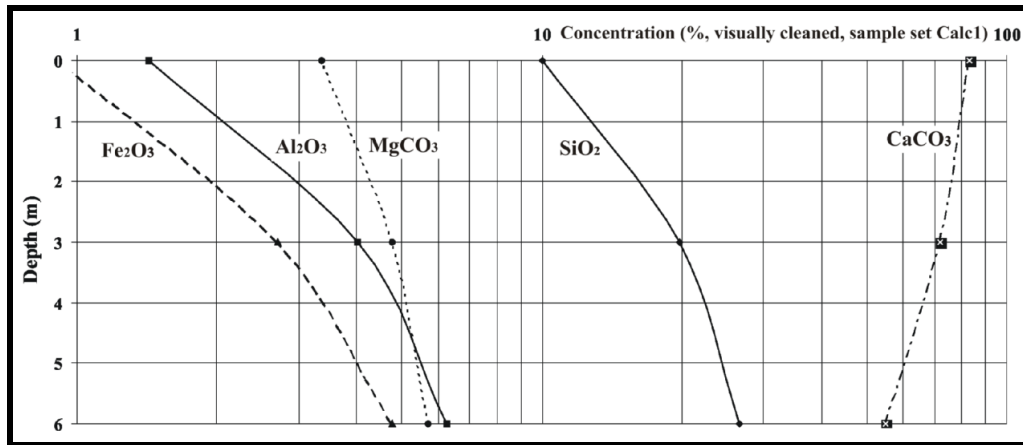


Figure 6. Major oxides variation versus depth in the Areachapcalcrete layer (visually cleaned samples referred to as Calc1).

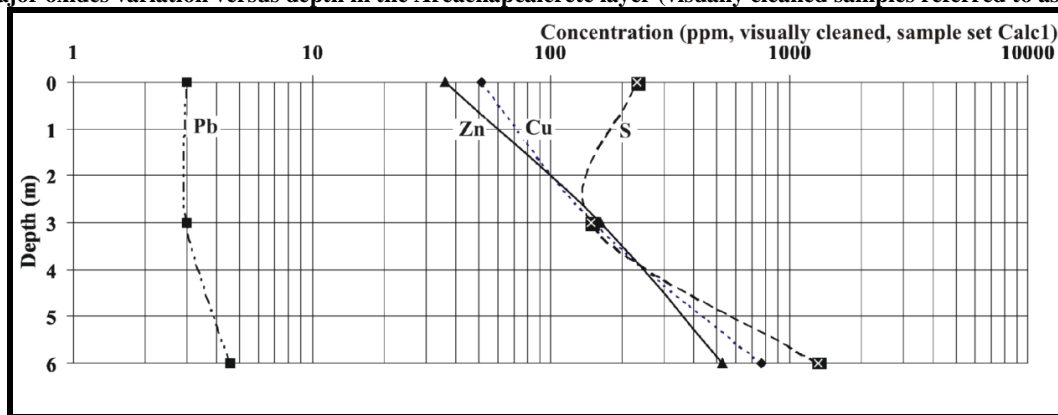


Figure 7. Variation of Cu, Zn, Pb and S versus depth in the Areachapcalcrete layer, (visually cleaned samples referred to as Calc1).

The variation of major oxides versus depth for the calcrete in sample set Calc2 in the Areachap area is shown (original samples) in Figure 8. The variation of CaCO₃ versus depth in compare to the other component is the same as calcrete sample set Calc1. They contain 48.89 to 63.89 % CaCO₃, 8.12 to 25.8 % SiO₂, 1.41 to 11.36 % Fe₂O₃, 1.68 to 7.3 % Al₂O₃ and 3.22 to 6.55 % MgCO₃ contents based on semi-quantitative XRF powder analyses.

The variations of trace elements in the original samples are demonstrated in Figure 9 (for sample set Calc2) as determined by quantitative (Cu, Zn and Pb) and semi-quantitative (S) XRF analyses. Based on this figure, Zn and Pb contents increase

with depth, but Cu and S contents decrease. The highest content of S occurs at the surface and the lowest content at a depth of 4 m. Trace elements, such as Pb and Zn, and major oxides, i.e. Al₂O₃, MgCO₃, SiO₂ and Fe₂O₃ show the same trend. Therefore the concentration of trace elements in calcrete samples at the surface depends on the thickness of the calcrete layer in the area.

5. Comparison of calcretes close to the ore zone and further away

In this section the composition of calcrete samples collected from above the ore zone (anomalous samples, Calc1-3 and Calc2-3) are compared to

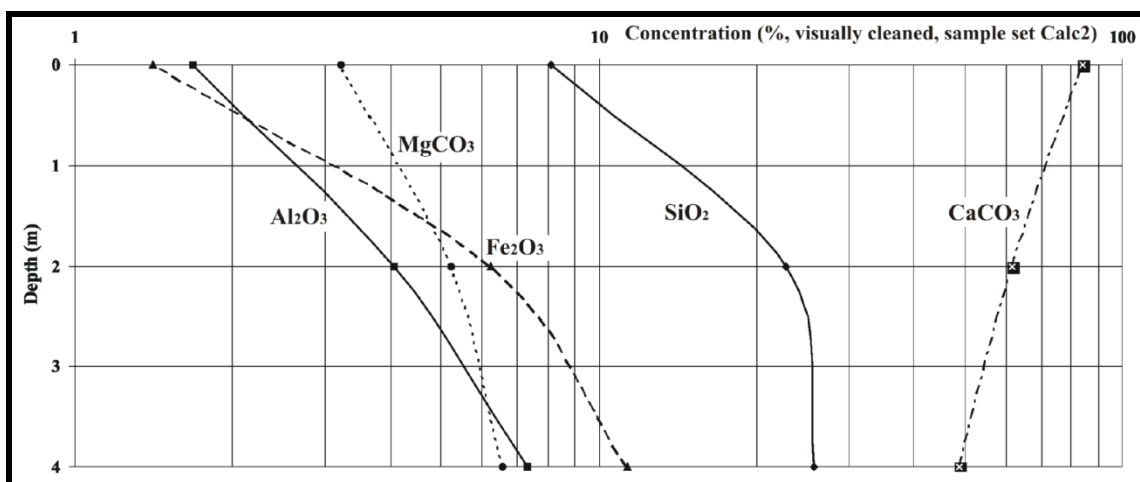


Figure 8: Major oxides variation versus depth (visually cleaned samples referred to as Calc2) in the Areachap.

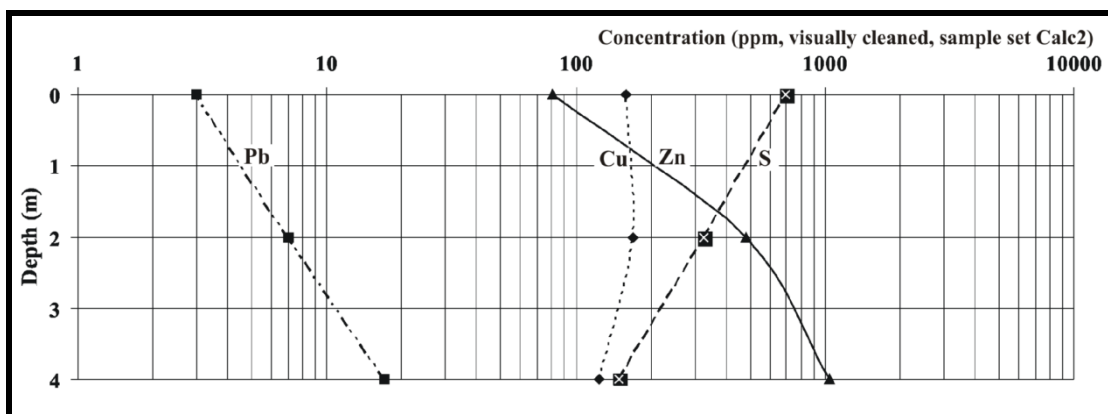


Figure 9: Variation of Cu, Zn, Pb and S versus depth in the calcrete layer, Areachap (visually cleaned samples referred to as Calc2).

samples (Vcal2 and Vcal3) that were collected away from any known mineralization (background samples). XRF results of these samples are given in Table A.3. Some of the calcrete samples provided by Vermaak (1984) from Areachap and Copperton Cu-Zn Mine and further away from the known mineralization (Table A.4) are also used here. These samples consist of the calcrete and complex calcrete, which are calcrete samples that contain gossan particles. The average values of the elements and oxides for these samples are used for plotting in the three angular diagrams.

In Table 5, the chemical composition of the original calcrete samples near the ore zone in the study area is compared to calcrete samples further away from the ore zone (at Kantienpan area). In Figure 10, the chemical composition of original calcretes above the ore zone and data set of Vermaak (1984) is compared to that of those samples collected further away from the known mineralization. Based on this figure, the calcrete samples near the ore zone are enriched in CaCO₃, Cu and Zn and samples collected further away from the known mineralization are enriched in V and Sr. The latter samples have higher Na₂O and K₂O contents when compared to the calcrete samples close to the ore zone. Calcretes directly related to massive sulphidemineralization may be discriminated from those developed in areas away from the mineralization by plotting the V-Cu-Zn and Sr-Cu-Zn contents in triangular diagrams as presented in Figure 10, A and B.

6. Conclusion

The calcrete from the studied areas consists of a gossan bearing magnetic and calcite rich non-magnetic part. Based on quantitative XRD analyses of these two parts, it is concluded that magnetite and hematite are concentrated in the magnetic fractions, calcite, albite, microcline and quartz are more abundant in the non-magnetic fractions. Calcite is present in both the magnetic and non-magnetic fractions of the sample due to poor liberation during grinding. The distribution of trace elements, especially Cu and Zn, are strongly related to the distribution of magnetite (the magnetic part of the sample) although some of the Cu and Zn are also dispersed in the non-magnetic "cleaned" fractions of the sample. Pb and V are directly associated with the distribution of magnetite.

The variation of the elements of interest in the visually cleaned calcrete shows that the

concentrations of Cu, Zn and Pb are much lower at, and near the surface than deeper down within the calcrete profiles. The concentrations of these elements that could be expected in calcrete at the surface and the peak to background ratio of anomalies at surface will therefore depend on the thickness of the underlying calcrete layer in the area.

S, as a trace element, does not show the same trend as Cu, Zn and Pb. This may be explained by the presence of different types of sulphur-bearing phases in the sample, i.e., sulphates that form as a result of ground water compositions and evaporation processes, or sulphates that form as remnants after the oxidized primary sulphide minerals. The former may result in false S anomalies not related to underlying sulphide mineralization.

The calcrete layer shows the signature of mineralization even though the size of the halo is only restricted to the ore zone. Calcretes directly related to massive sulphide mineralization may be discriminated from those developed in areas away from the mineralization by plotting the Sr-Cu-Zn and V-Cu-Zn contents in triangular diagrams. The original calcrete samples near the ore zone are enriched in CaCO₃, Cu and Zn. Those samples collected further away from the known mineralization are enriched in V, Sr and MgCO₃ and have higher Na₂O, K₂O and SiO₂ contents.

Acknowledges

We are grateful to Prof S.A. de Waal for the financial support from the Centre for the Research of Magmatic Ore Deposits. Thanks are also due to Mr. D. Rossouw. M Classen for accompany in field visits. Thanks must also be given to Mrs. M. Loubser for analyzing samples by XRF. We also wish to thank Miss. I. Chimeloan for drafting some of the geological maps.

References

- [1]. Vermaak, J. J. (1984). Aspects of the secondary dispersion of ore-related elements in calcrete-environments of the Northern Cape Province. Unpublished M.Sc. thesis, University of the Orange Free State, Bloemfontein, 549.1145 VER.
- [2]. Ringrose, S., Downey, B., Genecke, D., Sefe, F. and Vink, B. (1999). Nature of sedimentary deposits in the Western Makgadikgadi basin, Botswana. *J ARID ENVIRON*, 43: 375-397.

Table 5 Chemical composition of visually cleaned calcretes near the ore zone (Calc1-3 and Calc2-3 at Areachap) and further away from the mineralized zone (Vcal2 and Vcal3)

| Major oxides (%) | Original | Original | Original | Original |
|----------------------|----------|----------|----------|----------|
| | calc1-3 | Calc2-3 | Vcal2 | Vcal3 |
| SiO2 * | 10.01 | 8.12 | 18.2 | 12.9 |
| MgCO3 * | 3.36 | 3.22 | 7.44 | 7.44 |
| CaCO3 * | 83.34 | 83.89 | 69.64 | 76.25 |
| Na2O * | 0.14 | 0.19 | 0.3 | 0.2 |
| K2O * | 0.25 | 0.33 | 0.5 | 0.4 |
| Trace elements (ppm) | | | | |
| Cu | 52 | 159 | 2 | 2 |
| Pb | 3 | 3 | 3 | 3 |
| Sr | 114 | 158 | 149 | 236 |
| Zn | 36 | 81 | 29 | 30 |
| S * | 229 | 699 | 294 | 231 |
| Sc | 1 | 1 | <1 | <1 |
| V | 19 | 28 | 24 | 41 |
| Depth | Surface | Surface | Surface | Surface |

*: Semi-quantitative analysis

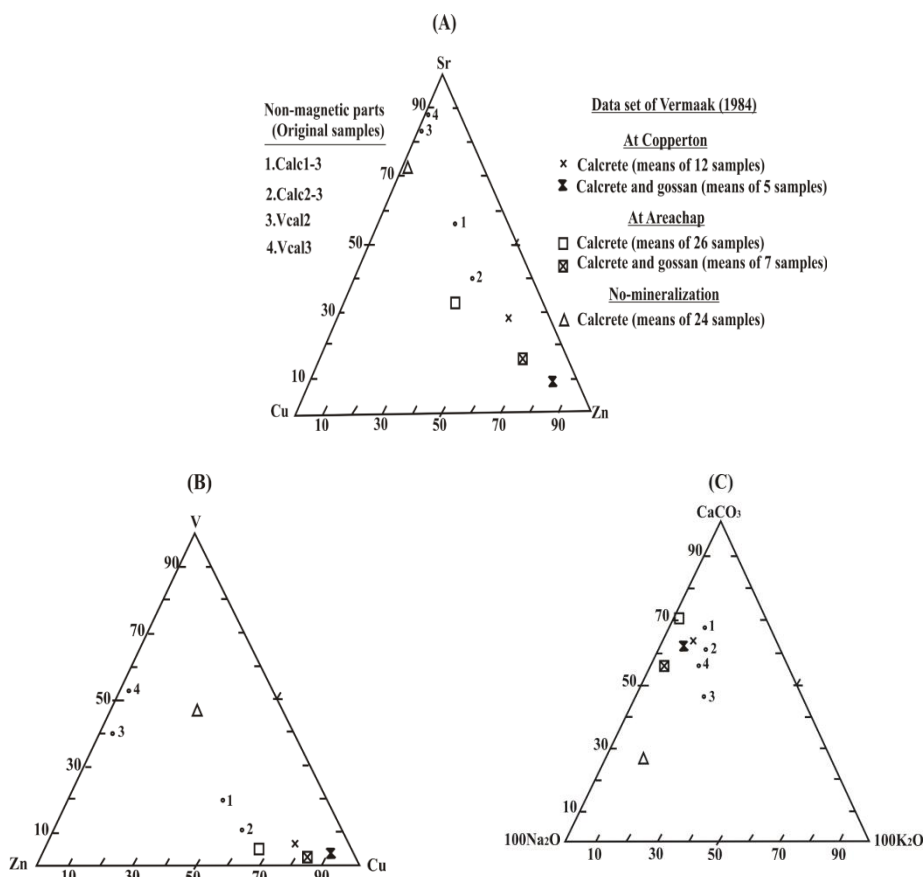


Figure 10. Variation of trace elements (A and B) and major components (C) of calcrete samples close to ore deposit and further away from the mineralized zone.

- [3]. Jimenez-Espinosa R. and Jimenez-Millan J. (2003). Calcrete development in Mediterranean colluvial carbonate systems from SE Spain. *Journal of Arid Environments*, 53: 479-489.
- [4]. Khadkikar, A.S., Merh, S.S., Malik, J.N. and Chamyal, L.S. (1998). Calcretes in semi-arid alluvial systems: formative pathways and sinks. *SEDIMENT GEOL*, 116: 251-260.
- [5]. Khadkikar, A.S., Chamyal, L.S. and Ramesh, R. (2000). The character and genesis of calcrete in Late Quaternary alluvial deposits, Gujarat, western India, and its bearing on the interpretation of ancient climates. *PALAEOGEOGR PALAEOCL*, 162: 239-261.
- [6]. Cameron, E.M., Hamilton, S.M., Leybourne, M.I. and Hall, G.E.M. (2004). Finding deeply buried deposits using geochemistry. *GEOCHEM-EXPLOR ENV A*, 4: 7-32.
- [7]. Mann, A.W., Birrell, R.D., Fedikow, M.A.F. and De Souza, H.A.F. (2005). Vertical ionic migration: mechanisms, soil anomalies, and sampling depth for mineral exploration. *GEOCHEM-EXPLOR ENV A*, 5: 201-210.
- [8]. Mann, A.W., Birrell, R.D., Perdrix, J.L., Mann, A.T., Humphreys, D.B. and Gry, L.M. (1995). Project M219: Mechanism of formation of mobile metal ion anomalies. Meriwa report No. 153, Perth, W.A., 407 pp.
- [9]. Mann, A.W., Mann, A.T., Humphreys, D.B., Dowling, S.E., Staltari, S. and Myers, L. (1997). Soil geochemical anomalies-their dynamic nature and interpretation. Meriwa report No. 184, Perth., 132 pp.
- [10]. Thomas, M.A. (1981). The geology of the Kalahari in the northern Cape Province (Areas 2620 and 2720). Unpublished M.Sc. thesis, University of the Orange Free State, Bloemfontein.
- [11]. Ward, J.D., Seely, M.K. and Lancaster, I.N. (1983). On the antiquity of the Namib. *South AFR J SCI*, 79: 175-183.
- [12]. Ghavami-Riabi, R., Theart, H.F.J., De Jager, C. (2008). Detection of concealed Cu-Zn massive sulfide mineralization below eolian sand and a calcrete cover in the eastern part of the Namaqua Metamorphic Province, South Africa. *J. Geochem. Explor.* 97: 83-101.
- [13]. Malherbe, S.J. (1984). The geology of the Kalahari Gemsbok National Park. *Proceedings of a Symposium on the Kalahari Ecosystem*, 33-44.
- [14]. Nash, D.J. and McLaren, S.J. (2003). Kalahari valley calcretes: their nature, origins, and environmental significance. *QUATERN INT*, 111: 3-22.
- [15]. Voet, H.W. and King, B.H. (1986). The Areachap copper-zinc deposit, Gordons district., In: S. Maske (Editors) *Mineral Deposits of southern Africa*, *GEOL SOC S Afr*, 2: 1529 pp.
- [16]. Rossouw, D. (2003). A technical risk evaluation of the Kantiapan volcanic-hosted massive sulphide deposit and its financial viability. Unpublished M.Sc. thesis, University of Pretoria, 118 pp.
- [17]. McQueen, K.G.; Hill, S.M. and Foster, K.A. (1999). The nature and distribution of regolith carbonate accumulations in southeastern Australia and their potential as a sampling medium in geochemical exploration. *Journal of Geochemical Exploration*, 67, 67-82.
- [18]. Dart, R. C. (2009). Gold-in-calcrete: a continental to profile scale study of regolith carbonates and their association with gold mineralisation. Thesis (Ph.D.) - University of Adelaide, School of Earth and Environmental Sciences, 299p.
- [19]. Bowell, R.J.; Barnes, A.; Grogan, J. & Dey, M. (2009). Geochemical controls on uranium precipitation in calcrete palaeochannel deposits of Namibia. *SRK Company, Wales*.
- [20]. Lintern, M. ; Hough, R. ; Ryan, C. (2012). Experimental studies on the gold-in-calcrete anomaly at Edoldeh Tank Gold Prospect, Gawler Craton, South Australia. *Journal of Geochemical Exploration*, Vol. 112, 189-20.

Appendix

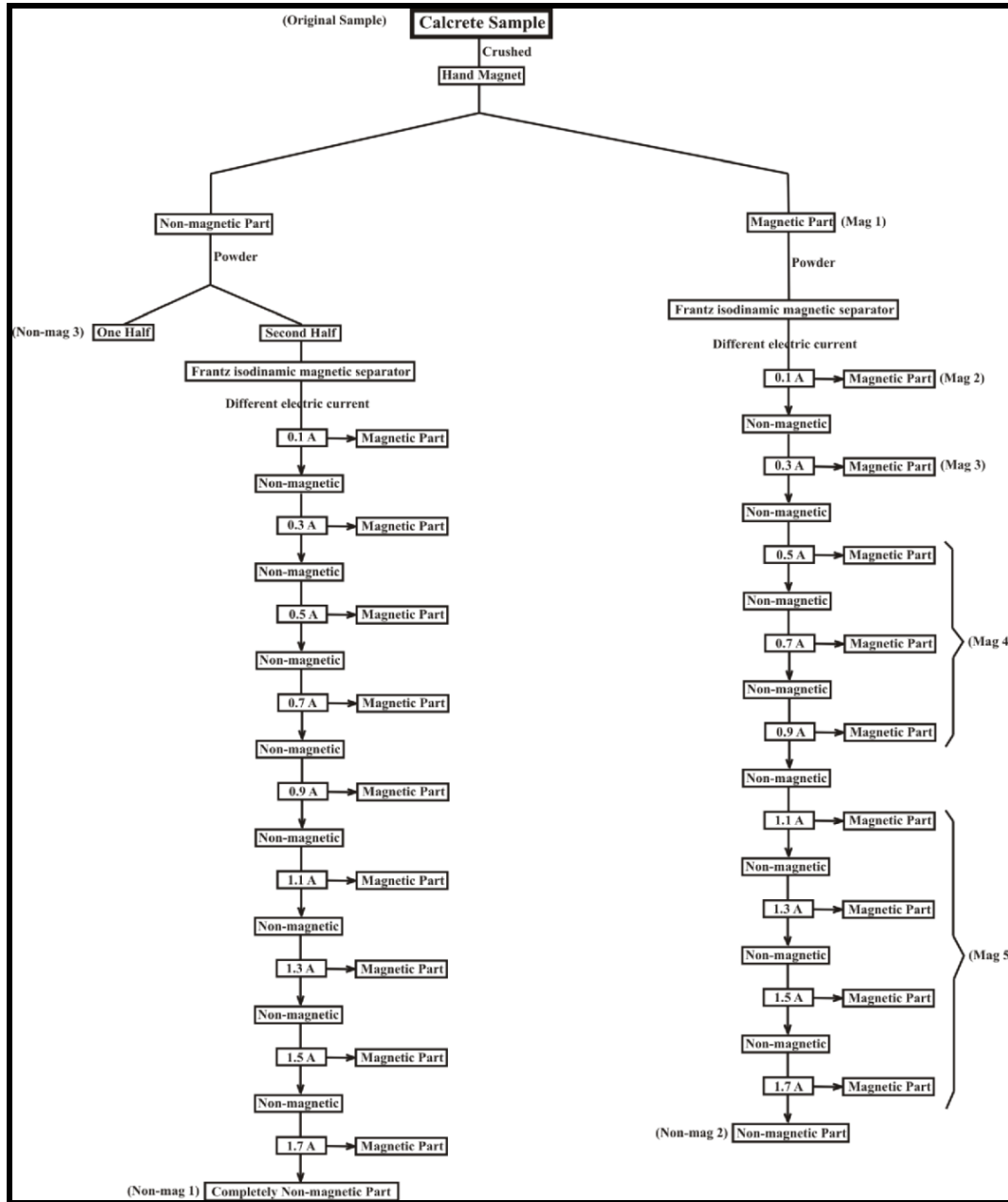


Figure A.1. Flow chart of the separation of magnetic and non-magnetic parts of calcrete samples [(in bracket): sample number for XRF analysis, A: ampere].

Table A.2. XRF results of the magnetic, non-magnetic and visually cleaned parts of the calcrete sample KPR12/4, Kantiapan (major elements: wt. %)

| % | KPR 12/4 | Non-Mag1 | Non-Mag2 | Non-Mag3 | Mag1 | Mag2 | Mag3 | Mag4 | Mag5 |
|--------------|--------------|--------------|--------------|--------------|--------------|--------------|--------------|--------------|--------------|
| SiO2 * | 18.43 | 16.84 | 13.84 | 15.56 | 12.67 | 12.71 | 12.42 | 13.79 | 14.69 |
| TiO2 * | 0.22 | 0.09 | 0.1 | 0.15 | 0.21 | 0.51 | 1.1 | 0.98 | 0.53 |
| Al2O3 * | 2.54 | 1.99 | 1.91 | 2.05 | 1.91 | 1.92 | 1.94 | 2.35 | 2.66 |
| Fe2O3 * | 1.52 | 0.74 | 0.74 | 1 | 1.61 | 9.99 | 3.2 | 3.3 | 2.14 |
| MnO * | 0.05 | 0.04 | 0.04 | 0.05 | 0.04 | 0.06 | 0.08 | 0.08 | 0.06 |
| MgO * | 2.23 | 2.10 | 2.04 | 2.19 | 2.12 | 2.35 | 2.14 | 2.34 | 2.43 |
| CaO * | 39.34 | 39.81 | 42.0 | 39.96 | 42.42 | 39.92 | 40.77 | 40.73 | 40.58 |
| Na2O * | 0.23 | 0.24 | 0.24 | 0.23 | 0.23 | 0.27 | 0.27 | 0.28 | 0.28 |
| K2O * | 0.71 | 0.66 | 0.58 | 0.64 | 0.57 | 0.41 | 0.44 | 0.49 | 0.56 |
| P2O5 * | 0.17 | 0.21 | 0.11 | 0.22 | 0.11 | 0.09 | 0.09 | 0.12 | 0.17 |
| TOTAL | 65.44 | 62.72 | 61.57 | 62.04 | 61.90 | 68.23 | 62.46 | 64.45 | 64.10 |

Note: KPR12/4 is the original sample, Non-Mag: non-magnetic part of sample; Mag: magnetic part of samples.

*: Semi-quantitative XRF powder analyses

Table A.2. Continued

| Trace elements (ppm) | KPR 12/4 | Non-Mag1 | Non-Mag2 | Non-Mag3 | Mag1 | Mag2 | Mag3 | Mag4 | Mag5 |
|----------------------|----------|----------|----------|----------|------|------|------|------|------|
| As | 9 | 12 | 8 | 5 | 6 | 16 | 8 | 11 | 6 |
| Cu | 20 | 12 | 8 | 12 | 5 | 6 | 11 | 14 | 13 |
| Ga | 2 | 2 | 2 | 2 | 2 | 3 | 2 | 2 | 2 |
| Mo | 1 | 1 | 1 | 1 | 1 | 1 | 1 | 1 | 1 |
| Nb | 4 | 2 | 3 | 3 | 5 | 6 | 13 | 10 | 7 |
| Ni | 6 | 4 | 4 | 5 | 4 | 9 | 5 | 8 | 9 |
| Pb | 4 | 3 | 3 | 6 | 3 | 16 | 3 | 4 | 3 |
| Rb | 24 | 20 | 19 | 20 | 19 | 16 | 18 | 18 | 22 |
| Sr | 180 | 218 | 242 | 219 | 240 | 233 | 233 | 237 | 238 |
| Th | 4 | 4 | 3 | 6 | 5 | 4 | 3 | 6 | 6 |
| U | 3 | 3 | 3 | 3 | 3 | 3 | 3 | 3 | 3 |
| W * | 82 | 156 | 104 | 68 | 54 | 6 | 11 | 19 | 22 |
| Y | 10 | 8 | 8 | 9 | 8 | 9 | 10 | 16 | 16 |
| Zn | 45 | 42 | 39 | 52 | 42 | 70 | 86 | 68 | 62 |
| Zr | 85 | 69 | 73 | 87 | 76 | 65 | 94 | 90 | 92 |
| Cl * | 552 | 528 | 287 | 486 | 441 | 172 | 197 | 174 | 197 |
| Co | 9 | 9 | 4 | 2 | 2 | 31 | 3 | 5 | 3 |
| Cr | 10 | 10 | 10 | 10 | 10 | 10 | 10 | 10 | 10 |
| F * | 268 | 491 | 274 | 471 | 419 | 100 | 1452 | 560 | 651 |
| S * | 513 | 578 | 363 | 1142 | 446 | 289 | 300 | 299 | 329 |
| Sc | 1 | 1 | 1 | 1 | 1 | 1 | 1 | 1 | 1 |
| V | 35 | 16 | 18 | 19 | 37 | 305 | 72 | 63 | 46 |

Note: KPR12/4 is the original sample, Non-Mag: non-magnetic part of sample; Mag: magnetic part of samples.

*: Semi-quantitative analyses

Table A.3. Chemical composition of calcretes near the ore zone (Calc1-3 and Calc2-3, Areachap area) and further away from ore zone (Vcal2 and Vcal3, Kantienpan area)

| % | Original | Original | Original | Original |
|---------|----------|----------|----------|----------|
| | Calc1-3 | Calc2-3 | Vcal2 | Vcal3 |
| SiO2 * | 10.01 | 8.12 | 18.20 | 12.90 |
| TiO2 * | 0.15 | 0.19 | 0.20 | 0.20 |
| Al2O3 * | 1.43 | 1.68 | 2.50 | 1.80 |
| Fe2O3 * | 0.91 | 1.41 | 1.10 | 1.40 |
| MnO * | 0.05 | 0.05 | 0.00 | 0.00 |
| MgCO3 * | 3.36 | 3.22 | 7.44 | 7.44 |
| CaCO3 * | 83.34 | 83.89 | 69.64 | 76.25 |
| Na2O * | 0.14 | 0.19 | 0.30 | 0.20 |
| K2O * | 0.25 | 0.33 | 0.50 | 0.40 |
| P2O5 * | 0.03 | 0.09 | 0.10 | 0.10 |
| TOTAL | 99.67 | 99.17 | 99.98 | 100.69 |
| ppm | calc1-3 | Calc2-3 | Vcal2 | Vcal3 |
| As | 5 | 11 | 9 | 6 |
| Cu | 52 | 159 | 2 | 2 |
| Ga | 2 | 2 | 2 | 2 |
| Mo | 1 | 1 | 1 | 1 |
| Nb | 2 | 3 | 3 | 3.7 |
| Ni | 3 | 3 | 6 | 6 |
| Pb | 3 | 3 | 3 | 3 |
| Rb | 14 | 14 | 18 | 16 |
| Sr | 114 | 158 | 149 | 236 |
| Th | 4 | 4 | 3 | 3.5 |
| U | 3 | 3 | 3 | 3 |
| W * | 14 | 6 | 44 | 9 |
| Y | 10 | 9 | 8 | 8 |
| Zn | 36 | 81 | 29 | 30 |
| Zr | 70 | 145 | 66 | 41 |
| Cl * | 8 | 40 | 102 | 8 |
| Co | 2 | 2 | 2 | 2 |
| Cr | 10 | 10 | 10 | 10 |
| F * | 177 | 310 | 100 | 366 |
| S * | 229 | 699 | 294 | 231 |
| Sc | 1 | 1 | <1 | <1 |
| V | 19 | 28 | 24 | 41 |

Note: *: Semi-quantitative analyses

Table A.4. Chemical composition of calcretes near and further away from ore zone analyzed by the XRF method (Vermaak, 1984).

| Vermaak Data set (1984) | | | | | |
|-------------------------|-------------------------|-----------------|------------------------|-----------------|-------------------|
| Major Oxides (%) | Copperton Cu-Zn deposit | | Areachap Cu-Zn deposit | | No Mineralization |
| | Calcrete | Complex samples | Calcrete | Complex samples | Average |
| No. of Samples | 12 | 5 | 26 | 7 | 24 |
| SiO2 | 21.18 | 29.24 | 20.00 | 24.71 | 28.94 |
| Fe2O3 | 2.75 | 11.35 | 1.29 | 12.89 | 1.82 |
| MgCO3 | 8.81 | 7.20 | 4.83 | 3.35 | 6.06 |
| CaCO3 | 61.46 | 52.09 | 67.72 | 52.80 | 53.43 |
| Na2O | 0.03 | 0.06 | 0.00 | 0.03 | 0.25 |
| K2O | 0.25 | 0.27 | 0.29 | 0.39 | 1.30 |
| Trace elements (ppm) | | | | | |
| Sr | 344 | 378 | 195 | 173 | 242 |
| V | 151 | 628 | 13 | 101 | 22 |
| Cu | 1850 | 20883 | 325 | 5945 | 14 |
| Zn | 372 | 1792 | 140 | 1018 | 13 |